Structure of Zr_2ON_2 by Neutron Powder Diffraction: The Absence of Nitride–Oxide Ordering

S. J. Clarke,*,[1] C. W. Michie,† and M. J. Rosseinsky†,[1]

School of Chemistry, University of Exeter, Stocker Road, Exeter, EX4 4QD, United Kingdom; and †Inorganic Chemistry Laboratory, University of Oxford, South Parks Road, Oxford, OX1 3QR, United Kingdom

The structure of the fluorite-related zirconium oxynitride Zr_2ON_2 has been refined against a combination of laboratory X-ray and time of flight neutron powder diffraction data. The structure is of the bixbyite (C-M_2O_3) type. The high symmetry of the powder diffraction pattern does not allow us to easily distinguish between fully ordered, fully disordered, or partially ordered anion models. However, Rietveld refinements against both high and medium resolution neutron powder diffraction data clearly favour a statistical distribution of oxide and nitride anions over a single crystallographic site which is contrary to the predictions of previous calculations. The space group is $Ia\overline{3}$ (No. 206), with $a = 10.13940(7)$ Å at 298 K and $Z = 16$. This symmetry and unit cell are retained at low temperatures ($a = 10.1250(1)$ Å at 4.5 K). Partial oxidation reveals the existence of a phase with N_2 molecules weakly bound and the stoichiometry $ZrO_2(N_2)_{0.028(1)}$. We also report the isostructural hafnium oxynitride Hf_2ON_2, ($Ia\overline{3}$ with $a = 10.0692(2)$ Å at 298 K as determined using laboratory X-ray diffraction data). © 1999 Academic Press

INTRODUCTION

One approach to the low-temperature stabilisation of the high-temperature form of ZrO_2 with the fluorite structure and high oxide ion mobility is aliovalent substitution of Zr^{4+} by Y^{3+} or Ca^{2+} (1). As well as stabilising the fluorite structure, this introduces anion vacancies enhancing the oxide ion conductivity. A second approach is to make an anion substitution of O^{2-} by N^{3-} to make a series of zirconium oxynitrides which will have anion vacancies according to $ZrO_{2-x}N_{2x/3}V_{x/3}$ and represent a solid solution between ZrO_2 and Zr_3N_4. This was originally explored by Gilles *et al.* (2) and has received more attention in the past few years, particularly from Lerch and co-workers (3–6). These materials have ordered anion vacancies at low temperatures. Ohashi *et al.* (7) showed that the ionic conductivities are very low when there is anion/vacancy ordering. At high temperatures, however, the vacancies are randomly

distributed and the ionic conductivity is similar to that of yttria doped zirconia at 1000°C (8). Thompson (9) suggested that, in addition to anion/vacancy ordering, there should be O/N ordering in zirconium oxynitrides. This has not, however, been confirmed experimentally. Gilles *et al.* (2) described three new phases: Zr_2ON_2, $Zr_7O_8N_4$, and $Zr_7O_{11}N_2$. The latter two phases, designated β and β', respectively, have rhombohedral superstructures of the fluorite structure. The β-phase, $Zr_7O_8N_4$, is built up of Bevan clusters which are formulated $Zr_7O_8N_4$ and which contain ordered anion vacancies. The β'-phase, $Zr_7O_{11}N_2$, is composed of Bevan clusters and Zr_7O_{14} units alternating along the [001] direction in the hexagonal setting of the unit cell. The Zr_7O_{14} clusters are related to the Bevan clusters, by filling of the anion vacancies. Lerch and co-workers (4, 5, 10) have identified a third β type phase designated β'' and with stoichiometry $Zr_7O_{9.2}N_{3.2}$ obtained by carbothermal nitridation at 1900°C. This phase contains four Bevan clusters stacked along the [001] direction separated by a Zr_7O_{14} unit. The issue of O/N ordering in the Bevan clusters and the incommensurate nature of some of the β-phase structures, particularly the β''-phase (5), has not been fully addressed in zirconium oxynitrides. Here we address the question of O/N ordering in the most nitride-rich zirconium oxynitride Zr_2ON_2, designated the γ-phase which has the cubic C-M_2O_3 bixbyite structure which is also fluorite related (11). Neutron diffraction is usually ideally suited to the question of O/N ordering as the two anions have very different scattering lengths: N = 9.36 fm, O = 5.81 fm. However in this case the high symmetry of the diffraction pattern makes it difficult to distinguish a cubic model in $Ia\overline{3}$ with a single anion site from an alternative orthorhombic model in $Ibca$ with partial or full anion order over three sites and a metrically cubic unit cell. Our Rietveld refinements suggest that there is no ordering between oxide and nitride anions. This is in contrast to the conclusion of other workers (6) reached using the results of Madelung energy calculations carried out on a structural model obtained from X-ray powder diffraction measurements.

[1]To whom correspondence should be addressed.

399

EXPERIMENTAL

Synthesis

Synthesis was carried out using the method of Gilles *et al.* (2). Low hafnia grade zirconia (ZrO_2, 99.99%, Aldrich Chemical Co.) was spread along the length of a 4 cm long alumina boat in a 22 mm internal diameter silica tube. The tube was placed inside a split tube furnace and ammonia (NH_3, 99.98%, British Oxygen Co.) used as supplied, was flowed at a rate of approximately 12 dm^3 hr^{-1} through the tube. The temperature was raised to between 950 and 1000°C at a rate of 7°C min^{-1} for periods of between 24 and 48 hours whence the flow tube was isolated from the ammonia flow and removed from the furnace so that the sample cooled to room temperature in a few minutes under a static atmosphere of ammonia. The flow tube was constructed so that there was no exposure of the sample to air while the sample was hot. When cool, the material is not air-sensitive and was handled in air. The phase purity was monitored using X-ray powder diffraction. During the reaction with flowing ammonia, the more nitride-rich phases form preferentially at the upstream end of the sample where the partial pressure of ammonia is greatest and the partial pressure of water is lowest. Thus, the 2 cm long zone of sample at the upstream end of the boat consisted of mainly the γ-phase, while the 2 cm zone at the downstream end consisted mainly of β-phases. It was necessary to regrind and reheat the sample 10 times in order to remove entirely the white oxide-rich β-phases and achieve purely the lemon-yellow γ-phase along the whole length of the sample. Although Zr^{IV} is quite resistant to reduction under these conditions, prolonged treatment at temperatures greater than 1000°C led to partial reduction of the sample at the extreme upstream end of the flow and the formation of a blue-grey Zr_xN phase (12) ($x \approx 0.9$) with the rock-salt structure (lattice parameter = 4.545(5) Å) which was removed mechanically. This restricted us to the synthesis of 0.6 g of Zr_2ON_2 which was phase pure by X-ray powder diffraction and which was used in this study. Subsequently we found that re-oxidation of a mixture of zirconium oxynitrides in air at 800°C results in very finely divided ZrO_2 which can be transformed to Zr_2ON_2 at temperatures as low as 800°C under flowing ammonia and thus without reduction of Zr^{IV} at the upstream end.

Chemical analysis was carried out by combustion and by full oxidation back to ZrO_2 in air using a Rheometric Scientific 1500H thermogravimetric balance.

X-Ray Powder Diffraction

Measurements were made using a Philips PW 1050/81 diffractometer operating in Bragg–Brentano geometry with $CuK\alpha_1/\alpha_2$ radiation and equipped with a diffracted beam monochromator. Data for Rietveld refinement were col-

lected in the 2θ range 5 to 110° with a step size of 0.02° and a count time of 7.7 seconds per point. High resolution X-ray powder diffraction data were obtained using a Siemens D5000 diffractometer operating in Bragg–Brentano geometry with monochromatic $CuK\alpha_1$ radiation (Ge(111) monochromator) and a scintillation counter detector. Soller slits placed before and after the sample combined with a 0.1 mm detector slit improved the resolution so that the peak widths were determined by the sample. The instrumental resolution in this configuration was approximately 0.05° full width at half maximum, as determined using a silicon standard.

Neutron Powder Diffraction

Time of flight data were collected on 0.6 g of material using the diffractometer POLARIS at the ISIS Facility, Rutherford Appleton Laboratory. We used ^3He tube detector banks at 35 and 145° and the ZnS scintillation detector bank at 90° to access an overall d-spacing range between 0.5 and 5 Å. The measurement was made for an integrated proton current at the production target of 560 µAhr at room temperature and 288 µAhr at 4.5 K (counting times of 3 and 1.5 hours, respectively). The sample was contained in a cylindrical 5 mm diameter, thin walled vanadium can sealed under 1 atm of He with an indium gasket. The 4.5 K data were obtained in an "ILL orange" cryostat. Data were also collected at room temperature using the high resolution powder diffractometer (HRPD) at ISIS on 0.6 g of material for an integrated proton current of 70 µAhr (2.5 hours). HRPD data were collected using the back-scattering bank (ZnS scintillation counter) at $2\theta = 168°$ in the d-spacing range 0.85 to 1.9 Å. Rietveld refinement of X-ray and neutron data was carried out using the general structure analysis system (GSAS) (13). We carried out Rietveld refinements against the HRPD data, against the laboratory X-ray data, and against all three POLARIS banks simultaneously. A combined refinement of the model against X-ray and POLARIS data simultaneously was weighted very heavily toward the neutron data and gave a result which was indistinguishable within error from the refinement against POLARIS data only.

RESULTS

Chemical Analysis

Chemical analysis by combustion indicated a 12.2(1)% by mass nitrogen content which corresponds to a stoichiometry of $Zr_2O_{1.03(2)}N_{1.98(2)}$. Thermogravimetric analysis indicated a composition of $Zr_2O_{1.09(2)}N_{1.94(2)}$.

Structure

Füglein *et al.* (6) synthesised Zr_2ON_2 by solid state reaction between Zr_3N_4 (99% obtained by ammonolysis of

ZrCl$_4$ (14)) and ZrO$_2$ (Alfa 99.9%) at 700°C. They refined the structure of Zr$_2$ON$_2$ using X-ray powder diffraction data and confirmed that the material is of the bixbyite type, isostructural with Tl$_2$O$_3$ (15) and α-Mn$_2$O$_3$ (16). These authors were unable to distinguish between nitride and oxide experimentally, but used the results of MAPLE (17) calculations to suggest possible reduction of symmetry from cubic $Ia\overline{3}$ with disordered anions to orthorhombic $Ibca$ with an almost metrically cubic unit cell and partially or fully ordered anions. The authors point out the similarity of the simulated neutron diffraction patterns of the ordered and disordered models. This is due to the fact that if orthorhombic, the cell must have axes of nearly equal length, and the resultant peak overlap obscures differences in the intensities of individual reflections in the cubic and orthorhombic models. Our simulations indicated that there are very small differences in the diffraction patterns at high d-spacing. We obtained an excellent agreement with all data sets using the fully disordered model in $Ia\overline{3}$ and the results of the X-ray and neutron refinements at 298 K and the neutron refinement at 4.5 K are presented in Table 1. The fit to the POLARIS data from the 145° data bank is shown in Fig. 1. However, model independent (Le Bail type (18)) fits to the data were fairly similar in $Ia\overline{3}$ and $Ibca$, (goodness of fit, χ^2 of 3.20 and 4.03, respectively) indicating that it might be difficult to distinguish the two models. Starting from the cubic $Ia\overline{3}$ model refined against the 145° POLARIS bank with a χ^2 of 2.91, we reduced the symmetry to $Ibca$ (atom positions in Table 2) and calculated χ^2 to be 4.05 prior to refinement of this model. An initial attempt to refine this orthorhombic model was carried out assuming full ordering of the anions over the three available sites. However, refinement of atomic positions or the lattice parameters or both resulted in unstable, nonconvergent refinements with standard deviations in the atomic positions and lattice parameters which were between one and two orders of magnitude greater than those of the same parameters in the
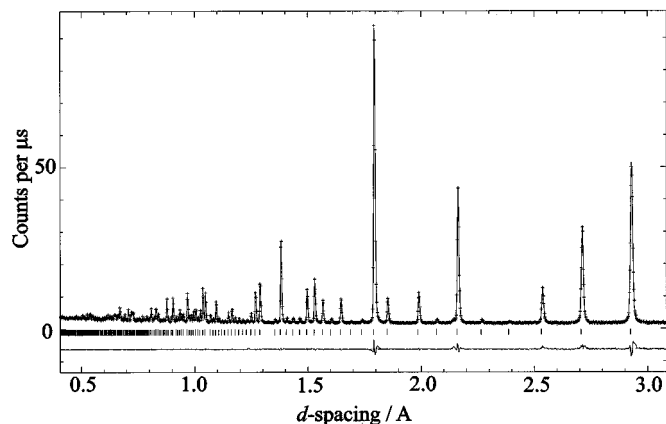

FIG. 1. The result of Rietveld refinement of Zr$_2$ON$_2$ against POLARIS data from the 145° detector bank collected at 298 K showing the data (dots), fit (line), and difference profile.

disordered model. The agreement factors of these refinements were also larger for the ordered model ($\chi^2 = 3.52$ and $R_{wp} = 0.020$ compared with values of 2.91 and 0.018, respectively, for the disordered model refined against the same data). Second, we started from a fully disordered orthorhombic model and allowed a degree of order to be introduced by carrying out an unconstrained refinement of the scattering length of each anion site. If the refinement was carried out so that the changes in scattering length were strongly damped, the refinement was stable and the refined values of the scattering lengths on each of the three anion sites had chemically sensible values. However, the large standard deviation in these parameters rendered the refined composition of Zr$_2$O$_{1(2)}$N$_{2(2)}$ almost meaningless. These standard deviations were at least two orders of magnitude larger than in the disordered case. Attempts to refine atomic positions, and subsequently the lattice parameters also, resulted in unstable nonconvergent refinements with very large standard deviations in the structural and cell parameters.

The atomic positions and zirconium-anion distances for the disordered $Ia\overline{3}$ model of Zr$_2$ON$_2$ refined against the

TABLE 1
Results of X-Ray and Neutron Refinements of Zr_2ON_2

Radiation	X-ray	Neutron	Neutron	Neutron
Instrument	Philips PW1050/81	POLARIS	HRPD	POLARIS
Temperature/K	298	298	298	4.5
Formula	Zr$_2$ON$_2$	Zr$_2$ON$_2$	Zr$_2$ON$_2$	Zr$_2$ON$_2$
Space group	$Ia\overline{3}$	$Ia\overline{3}$	$Ia\overline{3}$	$Ia\overline{3}$
Formula weight	226.5	226.5	226.5	226.5
a/Å	10.1415(1)	10.13940(7)	10.13277(4)	10.1250(1)
Volume/Å^3	1043.04(4)	1042.40(2)	1040.36(1)	1037.96(4)
ρ_{calc}/kgm^{-3}	5.768(1)	5.772(1)	5.783(1)	5.797(1)
No. of variables	20	49	26	60
χ^2	0.94	3.17	1.15	1.95
R_{wp}	0.109	0.0272	0.122	0.0113
R_p	0.0765	0.0436	0.0975	0.0181
$R(F^2)$	0.0326	0.0212	0.0772	0.0451

TABLE 2
Atomic Positions Appropriate to Ordered Anion Model in $Ibca$^{a}

Atom	Site	x	y	z
Zrl	8a	0	0	0
Zr2a	8c	0.2832	0	$\frac{1}{4}$
Zr2b	8d	$\frac{1}{4}$	0.2832	0
Zr2c	8e	0	$\frac{1}{4}$	0.2832
O/Na	16f	0.357	0.129	0.093
O/Nb	16f	0.093	0.357	0.129
O/Nc	16f	0.129	0.093	0.357

^{a}From Ref. (6).

TABLE 3
Atomic Positions for Zr_2ON_2

Data type		X-ray	Neutron	Neutron
Instrument		Philips PW1050	POLARIS	POLARIS
Temperature/K		298	298	4.5
Zr1	x	0	0	0
	y	0	0	0
	z	0	0	0
	$100 \times U_{iso}/Å^2$	0.75(5)	0.65(1)	0.59(4)
Zr2	x	0.2844(6)	0.28465(4)	0.2846(1)
	y	0	0	0
	z	0.25	0.25	0.25
	$100 \times U_{iso}/Å^2$	0.44(3)	0.44(1)	0.33(4)
O/N[a]	x	0.3583(4)	0.35813(3)	0.35806(8)
	y	0.1304(5)	0.13008(3)	0.12987(9)
	z	0.0968(4)	0.09678(3)	0.09675(9)
	$100 \times U_{iso}/Å^2$	0.2(1)	0.53(1)	0.36(4)

[a]Oxygen and nitrogen atoms with 1/3 and 2/3 occupancy, respectively, occupied a single site.

three POLARIS banks simultaneously are presented in Tables 3 and 4, respectively. Refinement of anisotropic displacement parameters for all three atoms indicated that the atoms were approximately isotropic at 298 K and 4.5 K. A Debye–Scherrer absorption correction using the functional form due to Hewat (19) made a significant improvement to the fit at long time of flight. If the cation and anion sites are all fully occupied, the composition must be Zr_2ON_2 because the Zr oxidation state is $+4$. We carried out an unconstrained refinement of the scattering length of the single occupied anion site; i.e., there was no requirement that the site should be fully occupied or that the oxidation state of Zr should be $+4$. This indicated a composition of $Zr_2O_{0.99(1)}N_{2.03(1)}$, which is consistent with the composi-

tion obtained by chemical analysis. However refinement of the composition had a very small effect on χ^2. We confirmed that there were no anions on the vacancy sites in this sample (the fractional occupancy of an atom placed on the vacant site at 0.13, 0.13, 0.13 refined to 0.00(2)). All three elements are strong coherent scatterers of neutrons and the neutron powder diffraction data have a better signal to noise ratio than the X-ray data, especially at small d-spacing because of a smaller fall-off of the nuclear scattering factor with decreasing d-spacing. Thus, as well as being weighted much more heavily than the X-ray data in a combined refinement, the neutron data gave much greater precision in the structural parameters.

A similar series of refinements was carried out on HRPD data. Although the counting statistics were poorer in this case the disordered model again refined stably ($\chi^2 = 1.15$, $R_{wp} = 0.122$). The orthorhombic ordered model did not refine stably and the estimated standard deviations were a factor of 10 larger than in the disordered case. Thus, all our Rietveld refinements strongly favour the disordered model with cubic symmetry. In addition, fitting of individual HRPD reflections using the program PKFIT1Vb (20) indicated that they could all be fit using a single peak. This is strongly indicative of the cubic disordered model especially in view of the extremely high resolution of HRPD ($\Delta d/d$ for this sample on HRPD was a constant 1.8×10^{-3} compared with a constant 4.2×10^{-3} on POLARIS). A similar treatment of the high resolution D5000 X-ray data ($\Delta d/d \approx 2 \times 10^{-3}$) indicated that the full-width at half-maximum (FWHM) of the peaks was less than the *spread* of the centers of the reflections contributing to a diffraction peak at high angle if the best orthorhombic refinement was assumed. In both the HRPD and D5000 high resolution diffraction data, reflections such as (044) (Fig. 2) and (004),
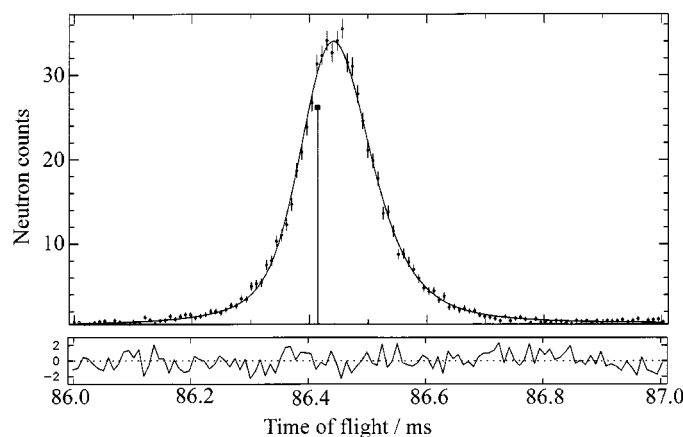
TABLE 4
Interatomic Distances in Å and Angles in Degrees for Zr_2ON_2

Zr1–O/N	×6	2.1845(4)	O/N–Zr1–O/N	×3	180
			O/N–Zr1–O/N	×6	99.758(8)
			O/N–Zr1–O/N	×6	80.242(8)
Zr2–O/N	×2	2.1497(4)	O/N–Zr2–O/N	×1	164.50(2)
Zr2–O/N	×2	2.1698(4)	O/N–Zr2–O/N	×1	139.84(2)
Zr2–O/N	×2	2.2345(4)	O/N–Zr2–O/N	×1	114.90(3)
			O/N–Zr2–O/N	×2	109.76(2)
			O/N–Zr2–O/N	×2	99.36(1)
			O/N–Zr2–O/N	×2	86.39(2)
			O/N–Zr2–O/N	×2	79.68(1)
			O/N–Zr2–O/N	×2	79.45(2)
			O/N–Zr2–O/N	×2	79.25(1)
O/N–Zr1	×1	2.1845(4)	Zr1–O/N–Zr2	×1	124.82(2)
O/N–Zr2	×1	2.1497(4)	Zr1–O/N–Zr2	×1	100.41(1)
O/N–Zr2	×1	2.1698(4)	Zr1–O/N–Zr2	×1	98.41(1)
O/N–Zr2	×1	2.2345(4)	Zr2–O/N–Zr2	×1	126.51(2)
			Zr2–O/N–Zr2	×1	100.21(2)
			Zr2–O/N–Zr2	×1	99.59(1)

FIG. 2. The (044) reflection ($d = 1.792$ Å) measured on HRPD and fitted to a single peak using the program PKFIT1Vb (20). This shows that the cubic model in $Ia\bar{3}$ is correct since no reduction in symmetry is indicated. d-spacing/Å = time of flight/ms $\times$ 0.0207 for HRPD.

which should be split in orthorhombic symmetry, were no broader than the (222) reflection which should be a single peak in both cubic and orthorhombic symmetry. In performing this analysis account was taken of the decrease in instrumental resolution with increasing 2θ for the D5000 X-ray diffractometer which was determined using a silicon standard. Thus, there is no direct evidence from the highest resolution diffraction data available that the cell is orthorhombic rather than cubic and this is consistent with our refinement results. If the symmetry is cubic $Ia\bar{3}$ then the anions must be statistically distributed over a single site since the orthorhombic $Ibca$ model is the highest symmetry one which allows ordering for the size of unit cell under consideration, and there are no superstructure reflections to indicate that a larger cell should be considered.

Oxidation

Thermogravimetric analysis (Fig. 3) indicates that oxidation to ZrO$_2$ is not complete until 1200°C. The mass of the sample at temperatures above 600°C is greater than that of the final ZrO$_2$ oxidation product. The partially oxidised material, cooled from 650°C in the TGA, is a poorly crystalline phase with the baddeleyite (monoclinic ZrO$_2$) structure. The source of the additional mass is N$_2$ molecules which are weakly bonded in the structure, presumably occupying the anion sites. The Raman spectrum (inset to Fig. 3) measured on a Dilor Labram spectrometer at a frequency of 632.82 nm showed a fairly strong resonance at 2329(1) cm^{-1} which is similar to the N$_2$ vibrational frequency in gaseous or liquid N$_2$ and confirms that N$_2$ moieties are present in the solid. Thermogravimetric analysis suggests a composition of ZrO$_2$(N$_2$)$_{0.028(1)}$ at 650°C. This nitrogen retention phenomenon has been observed previously in the oxidation of several oxynitrides (21). We have recently found that substitution of other metals, notably Ti, for Zr in the bixbyite structure oxynitrides leads to a 10-fold increase in the amount of N$_2$ retained on oxidation (22).
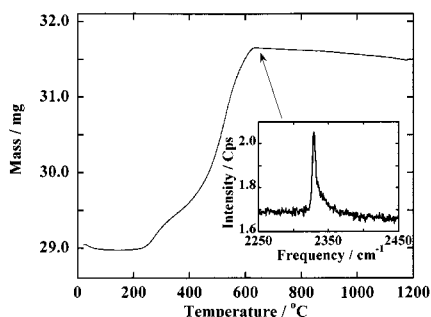

FIG. 3. The results of thermogravimetric analysis of Zr$_2$ON$_2$ showing that N$_2$ is retained during oxidation. The N$_2$ stretch measured by Raman spectroscopy is shown as an inset.
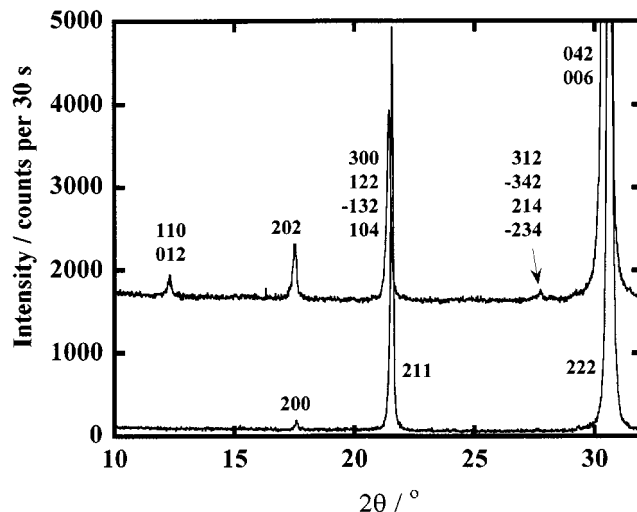

FIG. 4. The reduction in symmetry of the bixbyite structure from $Ia\bar{3}$ to $R\bar{3}$ as a result of filling up some of the vacant anion sites. The X-ray powder diffraction pattern of material with composition Zr$_7$O$_8$N$_4$ prepared at 720°C (upper) is compared with that of Zr$_2$ON$_2$ (lower). Indexing refers to a hexagonal cell in $R\bar{3}$ with $a = 14.3831(4)$ Å and $c = 17.5889(8)$ Å for Zr$_7$O$_8$N$_4$ and a cubic cell in $Ia\bar{3}$ with $a = 10.13951(2)$ Å for Zr$_2$ON$_2$. The data have been normalised so that the maximum intensities of the peaks at about 30.5° are equal at 40,000 counts per 30 s.

Solid Solution in the γ-Phase

Reaction of finely divided ZrO$_2$ with Zr$_2$ON$_2$ as a cold-pressed pellet in a sealed evacuated silica tube at between 700 and 750°C with the composition of the β-phase, Zr$_7$O$_8$N$_4$ produced a single phase which was clearly related structurally to the γ-phase Zr$_2$ON$_2$. This result is in keeping with the phase diagrams of Ohashi (7) and Lerch (8). This material, which is pale green in color, has the same-sized cell as Zr$_2$ON$_2$ but with lower symmetry. The symmetry of the Zr$_2$ON$_2$ structure is reduced from $Ia\bar{3}$ to $R\bar{3}$ as a result of filling some of the anion vacancies. This results in some additional weak superstructure reflections as shown in Fig. 4. The hexagonal lattice parameters are $a = 14.3831(4)$ Å and $c = 17.5889(8)$ Å. The structural details of this anion rich γ-phase are under investigation.

Hf$_2$ON$_2$

The greenish-grey hafnium analogue (23) was prepared in a similar manner to Zr$_2$ON$_2$. HfO$_2$ containing 1% ZrO$_2$ (Aldrich Chemical Co.) was reacted with ammonia at 950°C for 3 days and 980°C for 2 days with intermediate regrinding. In contrast to the zirconium case, there was no evidence for intermediate β-phases during synthesis. The structure was refined from laboratory X-ray data and showed Hf$_2$ON$_2$ to be isostructural with Zr$_2$ON$_2$, but with a slightly smaller cell parameter of 10.0692(2) Å. The refinement is
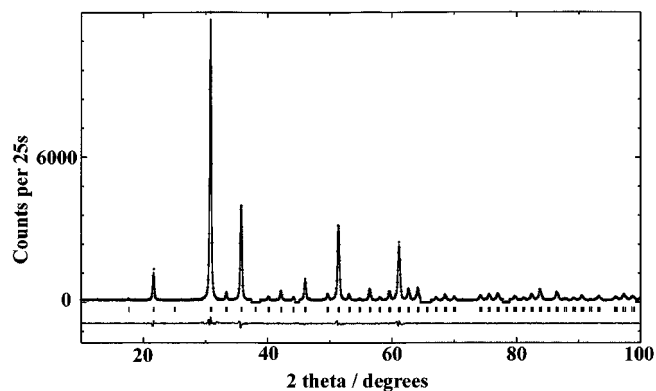
FIG. 5. The result of Rietveld refinement of the structure of Hf_2ON_2 against X-ray data at 298 K showing the data (dots), fit (line), and difference profile. Reflections due to the aluminum sample holder have been excluded from the refinement.

shown in Fig. 5, the refinement results are given in Table 5, and the atomic positions in Table 6. The Hf1-anion distance is 2.175(1) Å and the three Hf2-anion distances are 2.107(1), 2.182(1), and 2.217(1) Å.

DISCUSSION

The structure of Zr_2ON_2 is shown in Fig. 6. It is isostructural with α-Mn_2O_3 (16) and Tl_2O_3 (15). The interatomic distances and angles are listed in Table 4. There are two Zr sites which are shown in Fig. 7. Zr1, located at the origin, is surrounded by six anions in a distorted octahedral arrangement all at a distance of 2.1845(4) Å and has an isotropic thermal ellipsoid. Zr2 is in a much more distorted environment and is surrounded by six anions in three crystallographically distinct pairs. Two pairs of these are disposed approximately tetrahedrally about the Zr at distances of 2.1497(4) and 2.1698(4) Å. The other pair lie 2.2345(4) Å from Zr2 and are above the centres of two of the faces of the

TABLE 6
Atomic Positions for Hf_2ON_2

Data type		X-ray
Temperature/K		298
Hf1	x	0
	y	0
	z	0
	$100 \times U_{iso}/\text{Å}^2$	0.98(6)
Hf2	x	0.28385(7)
	y	0
	z	0.25
	$100 \times U_{iso}/\text{Å}^2$	0.52(3)
O/N[a]	x	0.3584(7)
	y	0.131(1)
	z	0.0954(7)
	$100 \times U_{iso}/\text{Å}^2$	0.5 (not refined)

tetrahedron described by the other four anions. The isotropic displacement parameter U_{iso} for Zr1 at 298 K is somewhat larger than that of Zr2, but this difference is entirely in keeping with the result obtained for Tl_2O_3 (15) and presumably reflects the slightly smaller size of the Zr2 site compared to the Zr1 site.

The results of MAPLE calculations (6) on the ordered $Ibca$ and disordered $Ia\bar{3}$ models indicated a stabilisation of 0.8% for the ordered model relative to the disordered model. Our results show, in contrast, that there appears to be no preference for any ordering. MAPLE calculations are probably not good at distinguishing between the two models as they do not take into account the covalent conributions to the bonding which will increase as the proportion of nitride anions increases. These calculations were based on a structural model for Zr_2ON_2 which was obtained using X-ray powder diffraction data. The precision in the atomic
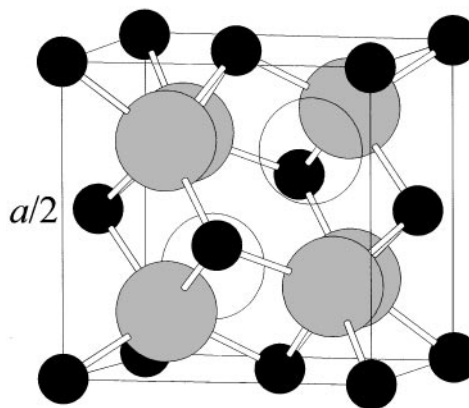
TABLE 5
Crystallographic and Refinement Data for Hf_2ON_2

Data	X-ray
Instrument	Philips PW1050/81
Temperature/K	298
Formula	Hf_2ON_2
Formula weight	400.99
Space group	$Ia\bar{3}$
$a/\text{Å}$	10.0692(2)
Volume/Å^3	1020.90(6)
ρ_{calc}/kgm^{-3}	10.436(1)
No. of variables	19
χ^2	3.58
R_{wp}	0.0686
R_p	0.0475
$R(F^2)$	0.0266

FIG. 6. One eighth of the unit cell of Zr_2ON_2 showing the relationship of this structure with that of fluorite. Small spheres are Zr, large spheres are anions. The ordered anion vacancies are represented by the large open circles.
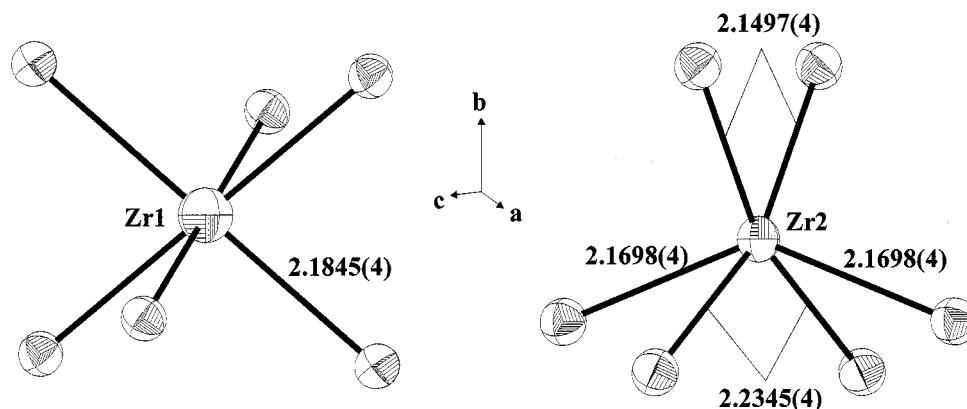
FIG. 7. The coordination geometries about the two Zr sites. Anisotropic displacement ellipsoids are shown at the 99.9% level.

positions is an order of magnitude greater for our measurement.

Zirconium oxynitrides are interesting in view of the high oxide ion conductivity which is shown by the yttria and calcia stabilised zirconias. The higher vacancy concentration in the oxynitrides could increase anion mobility, but appears only to do so at high temperatures where both the anions and the vacancies are disordered (7, 8). In these circumstances the ionic conductivity is comparable to that of the calcia and yttria stabilised materials. It is not yet known whether zirconium oxynitrides with disordered vacancies can be stabilised at low temperatures. The dimension of the fluorite subcell in Zr_2ON_2 is 5.07 Å (half of the dimension of the actual bixbyite cell). This is smaller than in the pure oxides: $Zr_{0.8}Y_{0.2}O_{1.9}$ (24) with the fluorite structure has a lattice parameter of 5.1473(1)Å.

REFERENCES

1. A. R. West, "Solid State Chemistry and Its Applications," p. 478. Wiley, Chichester, 1984.
2. J.-C. Gilles and R. Collongues, *C. R. Acad. Sci.* **254,** 1084 (1962).
3. M. Lerch, H. Boysen, and P. G. Radaelli, *J. Phys. Chem. Solids* **58,** 1557 (1997).
4. M. Lerch, *J. Am. Ceram. Soc.* **79,** 2641 (1996).
5. M. Lerch, F. Krumreich, and R. Hock, *Solid State Ionics* **95,** 87 (1997).
6. E. Füglein, R. Hock, and M. Lerch, *Z. Anorg. Allg. Chem.* **623,** 304 (1997).
7. M. Ohashi, H. Yamamoto, S. Yamanaka, and M. Hattori, *Mater. Res. Bull.* **28,** 513 (1993).
8. M. Lerch, *J. Mater. Sci. Lett.* **17,** 441 (1998).
9. D. P. Thompson, *Proc. 2nd ECRS, Augsburg,* 35 (1991).
10. D. Walter, M. Lerch, and W. Laqua, *J. Thermal Anal.* **48,** 709 (1997).
11. A. F. Wells, "Structural Inorganic Chemistry," 5th ed. Clarendon Press, Oxford, 1984.
12. R. Juza, A. Gabel, H. Rabenau, and W. Klose, *Z. Anorg. Allg. Chem.* **329,** 136 (1964).
13. A. Larson and R. B. von Dreele, "The General Structure Analysis System," Los Alamos National Laboratory, 1985.
14. M. Lerch, E. Füglein, and J. Wrba, *Z. Anorg. Allg. Chem.* **622,** 367 (1996).
15. H. H. Otto, R. Baltrusch, and H.-J. Brandt, *Physica C* **215,** 205 (1993).
16. S. Geller, *Acta Crystallogr. B* **27,** 821 (1971).
17. R. Hoppe, *Angew. Chem. Int. Ed.* **5,** 95 (1966).
18. A. Le Bail, *Mater. Res. Bull.* **23,** 447 (1988).
19. A. W. Hewat, *Acta Crystallogr. A* **35,** 248 (1979).
20. D. Sivia, unpublished.
21. L. LeGendre, R. Marchand, and Y. Laurent, *J. Eur. Ceram. Soc.* **17,** 1813 (1997).
22. S. J. Clarke, C. W. Michie, and M. J. Rosseinsky, in preparation.
23. A. Pialoux, *J. Nucl. Mater.* **200,** 1 (1993).
24. M. Yashima, S. Sasaki, M. Kakihana, Y. Yamaguchi, H. Arashi, and M. Yoshimura, *Acta Crystallogr. B* **50,** 663 (1994).